UNIVERSITY OF
TENNESSEE

Processing and Mechanical Behavior of Nicalon/SiC Composites with Sol-Gel Derived Oxide Interfacial Coatings

S. Shanmugham
P. K. Liaw

October 1996

Report prepared by
Department of Materials Science and Engineering
The University of Tennessee
434 Dougherty Engineering Bldg.
Knoxville, Tennessee 37996-2200

MASTER

under

for

Oak Ridge National Laboratory
Oak Ridge, Tennessee 37831
Managed by
LOCKHEED MARTIN ENERGY RESEARCH CORP.
for the
U.S. DEPARTMENT OF ENERGY

TABLE OF CONTENTS

DISCLAIMER

Portions of this document may be illegible
in electronic image products. Images are
produced from the best available original
document.

Processing and Mechanical Behavior of Nicalon®/SiC Composites with Sol-Gel Derived Oxide Interfacial Coatings

S. Shanmugham and P. K. Liaw

ABSTRACT

Recent analytical and finite element modeling (FEM) studies have indicated that low modulus interface materials are desirable for obtaining Nicalon/SiC composites with good toughness. Two oxides, aluminum titanate and mullite, were chosen on this basis as interface materials. The oxide and carbon (C) coatings were deposited by a sol-gel and a chemical vapor deposition process, respectively. Nicalon/SiC composites with oxide/C and C/oxide/C interfaces were fabricated and evaluated for flexure strength in the as-processed and oxidized conditions. Composites with C/oxide/C interfaces retained considerable strength and damage-tolerant behavior even after 500 h oxidation at 1000°C in air. The C/oxide/C interface shows promise as a viable oxidation-resistant interface alternative to C or BN interfaces.

® Ceramic Grade, Trade Mark of Nippon Carbon Company, Yokohama, Japan

1. INTRODUCTION

During the last few decades there has been a strong interest in developing advanced ceramic materials for high-temperature structural applications in the aerospace, defense, and automotive industry [1, 2]. Unfortunately, these materials lack significant stress-relieving mechanisms, and are inherently notch-sensitive and have low fracture toughness. To improve the strain and damage tolerance of ceramics, platelets, particles, whiskers, and continuous fibers have been introduced to create barriers to crack propagation [3-6]. The most dramatic improvement in toughness ($K_{IC} > 20$ MPa-$m^{0.5}$) has been obtained through reinforcement of continuous fibers in ceramic matrices [5, 6]. The Nicalon/SiC composite is one such system [6]. Most of the non-oxide and oxide continuous fibers are compiled in Tables 1 and 2, respectively, along with their important thermal and mechanical properties [7-12]. However, carbon, silica, and other glass fibers are not included in this compilation. This is because there are many manufacturers for these fibers.

It is widely accepted that the interface between the fiber and the matrix plays a key role in determining the composite properties [13-16]. A strong interface promotes effective load transfer between the fiber and the matrix, however, it will not arrest an impinging matrix crack, and the composite will exhibit brittle failure [Fig. 1 (a)]. In contrast, a weak interface will allow matrix crack deflection and promote energy absorption through several mechanisms: debonding at the fiber-matrix interface, crack deflection, fiber bridging, fiber fracture, and fiber slip and pullout [Fig. 1(b)]. Delamination is sometimes observed and is also shown in Fig. 1(b).

Currently, Nicalon/SiC composites owe their damage tolerance at room temperature to C or BN interfaces between the fiber and the matrix [13, 16]. However, C and BN interfaces are susceptible to oxidation at temperatures greater than 500°C and 900°C, respectively [16]. Consequently, composites with these interfaces undergo degradation of mechanical properties, either strength or toughness or both, within 100 h at 1000°C [17-19]. To overcome this limitation,

Table 1. Selected properties of commercially available non-oxide continuous ceramic fibers [7-12]

Trade Name	Manufacturer	Composition	Diameter (µm)	Density (g/cm³)	Tensile Strength (GPa)	Tensile Modulus (GPa)	CTE[^] $\times 10^{-6}$ (/°C)	ETF[^^] (%)	Filaments per yarn or tow	Availability and color	Process Type
SCS-6	Textron	β-SiC on C core	140	3	3.5-7	400	2.3	1	Monofilament	Commercial, Black	CVD^^
Sigma	BP	β-SiC+α-SiC on W core	100	3.4	3.4-4.1	400-410	-	0.8	Monofilament	Commercial	CVD^^
Nicalon (Ceramic grade)	Nippon Carbon	β-SiC + amorphous mixture of Si, C, O	15	2.55	3.0	192	3.9	1.5	500	Commercial, Black	Pyrolysis of polymer precursor
Nicalon (HVR grade)	Nippon Carbon	β-SiC + amorphous mixture of Si, C, and O	15	2.32	2.93	186	3.9	1.6	500	Commercial, Black	Pyrolysis of polymer precursor
Hi-Nicalon	Nippon Carbon	β-SiC + amorphous Si+C+O	14	2.74	2.8	270	-	1.0	500	Commercial, Black	Pyrolysis of polymer precursor
Tyranno (S grade)	Ube Industries	Amorphous Si+Ti+O+C	8.5, 11.0	2.35	3.2	170	3.1	1.9	800 and 1600	Commercial, Black	Pyrolysis of polymer precursor
MERX	MER	30-100% β-SiC+C	4-8	3	1-4.5	340-410	-	-	1000-12000	Limited, Greenish black	Chemical conversion of carbon
HPZ	Dow Corning	Amorphous Si+C+O+N	10	2.35	2.1-2.4	140-175	3	1	200-800	Discontinued	Pyrolysis of polymer precursor
MPDZ	Dow Corning	β-SiC + C+O+N	10-15	2.3	1.7-2.1	175-210	-	-	-	Discontinued	Pyrolysis of polymer precursor
MPS	Dow Corning	β/α SiC +O	10-15	2.6-2.7	1.0-1.4	175	-	-	-	Discontinued	Pyrolysis of polymer precursor
Tonen	Tonen	Amorphous Si+N+B	10	2.5	2.5	250	1.5	-	-	-	Pyrolysis of polymer precursor
Textron	Textron	B on W core	100 and 140	2.57	3.6	400	4.5	1	Monofilament	Commercial	CVD^^

^CTE - Coefficient of thermal expansion, temperature range not specified   ^^ETF - Elongation to failure   - indicates data not available to the author
^^^ CVD - Chemical vapor deposition

3

Table 2. Selected properties of commercially available oxide continuous ceramic fibers [7-12]

Trade Name	Manufacturer	Composition	Diameter (µm)	Density (g/cm³)	Tensile Strength (GPa)	Tensile Modulus (GPa)	CTE x10⁻⁶ (/°C)	ETF^^ (%)	Filaments per yarn or tow	Availability and color	Process Type
Saphikon	Saphikon	Al_2O_3 - 100%	125	3.97	2.1-3.4	386-435	7.9-8.8	11.5 ‖ to c axis	Monofilament	Commercial, Translucent	Melt grown
Fiber FP	Du Pont	Al_2O_3 > 99%	20	3.9	1.4	380	6.8	0.4	200	Discontinued, White	Slurry-spun
Almax	Mitsui Mining	Al_2O_3 > 99%	15	3.6	1.8	320	-	0.5	1000	Commercial, White	Slurry-spun
Nextel 610	3M	Al_2O_3 > 99% Fe_2O_3 - 0.4-0.7% SiO_2 - 0.2-0.3%	12	3.88	1.9	373	7.9	-	-	Commercial,	Sol-gel
Safimax	ICI	Al_2O_3 - 95% SiO_2 - 5%	3	3.3	2	300	-	-	Blanket	White	-
Altex	Sumitomo Chemical	Al_2O_3 - 85% SiO_2 - 15%	10, 15	3.3	1.8	210	8.8	0.8	500 and 1000	Commercial, White	Sol-gel
Nextel 720	3M	Al_2O_3 - 85% SiO_2 - 15%	12	3.4	2.1	260	6.0	-	-	Commercial,	Sol-gel
Nextel 550	3M	Al_2O_3 - 73% SiO_2 - 27%	12	3.03	2.0	193	5.3	-	-	Commercial,	Sol-gel
Nextel 440	3M	Al_2O_3 - 73% SiO_2 - 28% B_2O_3 - 2%	10-12	3.05	2.0	190	5.3	-	-	Commercial, Pink	Sol-gel
Nextel 312	3M	Al_2O_3 - 64% SiO_2 - 24% B_2O_3 - 14%	10-12	2.7	1.7	150	3	-	-	Commercial, White	Sol-gel
PRD-166	Du Pont	Al_2O_3 - 80% ZrO_2 - 20%	20	4.2	2.07	380	9	0.6	-	Discontinued, White	Slurry-spun
Nextel Z-11	3M	ZrO_2 - 68% SiO_2 - 32%	14	3.7	1.3	76	-	-	-	-	Sol-gel

^CTE - Coefficient of thermal expansion, temperature range not specified   ^^ETF - Elongation to failure   - indicates data not available to the author
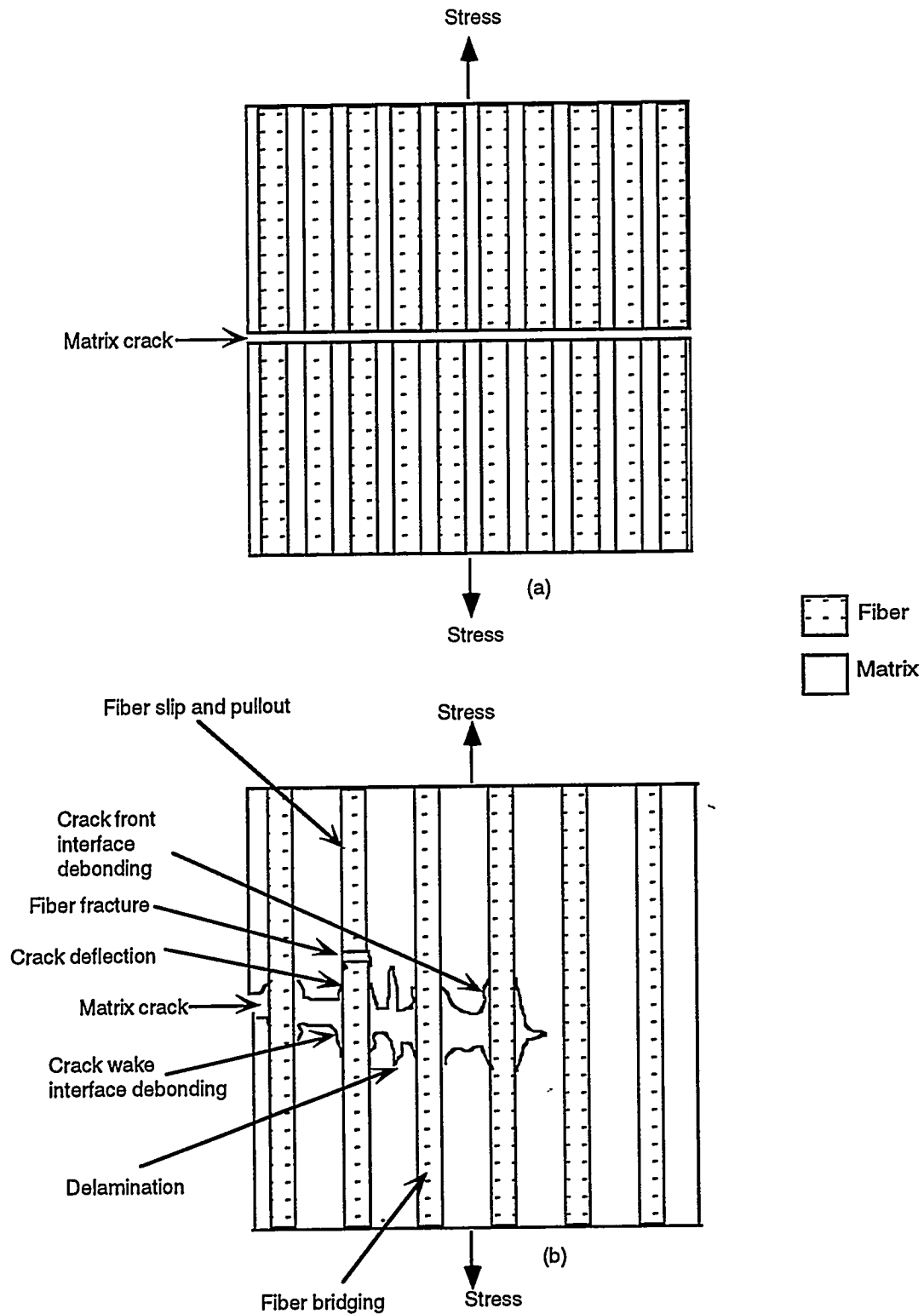
4

Fig. 1 Effect of interface bond on the failure of a ceramic matrix composite
(a) strong interface (b) weak interface

several interface materials, such as silicon, boron, molybdenum, boron-doped C, alumina, zirconia, and titania, have been investigated for attaining high-strength and high-toughness composites at elevated temperatures [15, 20-22]. However, there has been limited success.

Generally, metal oxides are inherently stable in air and possess thermal expansion coefficients relatively close to those of Nicalon and SiC. Hsueh et al. [23] indicated that a low-modulus interfacial coating would be effective in reducing the radial stresses that result upon cooling from processing to room temperature in composites, where the fiber has a lower thermal expansion coefficient than the matrix, and enhance fiber pullout. The FEM results of Shanmugham et al. [15] were similar to the analytical modeling predictions of Hsueh et al. [23]. Accordingly, the objective of the present study is to investigate the above hypothesis, with aluminum titanate (E = 20 GPa, a low modulus material) and mullite (E = 140 GPa, a moderate modulus material) as interface materials.

2. METHODOLOGY AND OXIDE INTERFACE CONCEPT

A Nicalon/SiC composite with a sol-gel derived mullite interface (50 nm thick) has been previously described (Fig. 2) [24]. However, this composite exhibited brittle fracture and could be attributed to the degradation of the Nicalon fibers during the sol-gel processing of the oxide. Hence, there is a need to apply an inert material between the fiber and oxide during the oxide deposition. For this purpose, a thin inner C coating (< 50 nm thick) was chosen. Thermodynamic modeling studies performed by Walukas [22] indicated that oxide coatings of alumina, titania, and zirconia would be attacked by HCl, a by-product of the SiC matrix formation reaction. To prevent the HCl attack on the oxide coating, an inert material between the oxide and SiC is desirable. Hence, a thin outer C coating (< 50 nm thick) was deposited. Earlier, Lowden [19] noted that such thickness of the C layer in a Nicalon/SiC composite would not produce good mechanical properties.
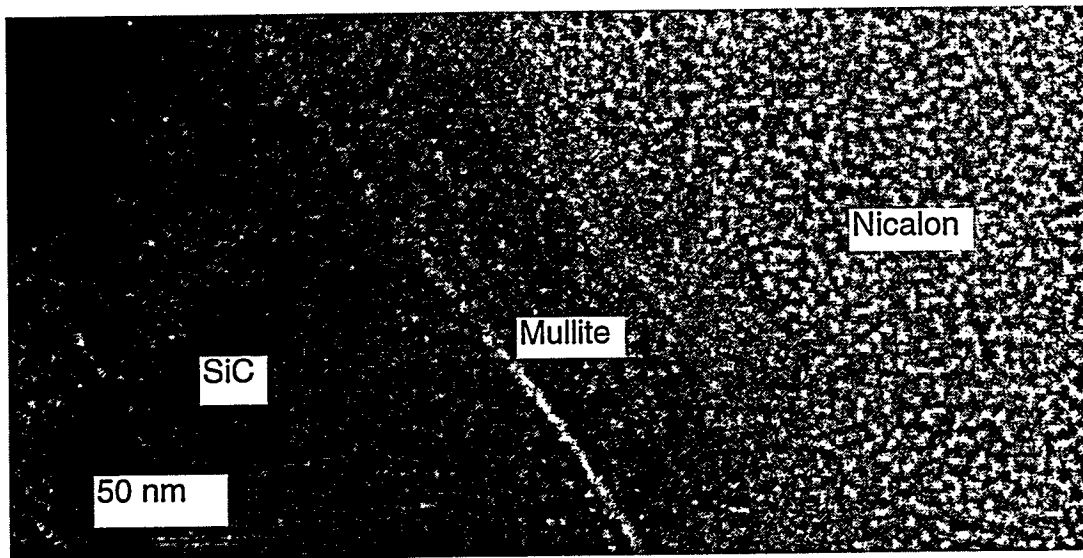
6

Fig. 2 TEM image of a Nicalon/SiC composite with a mullite interface.

Two different interfaces were considered for Nicalon/SiC composites: oxide/C and C/oxide/C. A composite with a C/oxide/C interface is termed as a composite with an oxide interface concept as shown in Fig. 3. For the oxide/C interface, the oxide is adjacent to the fiber and the C is between the oxide and the matrix. While in the C/oxide/C interface, the C on the extreme left is adjacent to the fiber, and the C on the extreme right is before the matrix. The oxide/C interface would be able to identify the degradation of the fiber, if any, during the sol-gel processing of the oxide. While in the C/oxide/C interface, the fiber is protected during the oxide deposition by the sol-gel method. To investigate the effect of modulus and the significance of the protection of the fiber during the sol-gel processing of the oxide on the composite properties, Nicalon/SiC composites with the following interfaces were fabricated: (1) mullite/C, (2) alumina-titania/C, (3) C/mullite/C, and (4) C/alumina-titania/C.

3. EXPERIMENTAL PROCEDURE

3.1. Mullite and Aluminosilicate Precursor Sols

The procedure used for the preparation of the mullite precursor sol has been slightly modified from that of Yoldas [25]: The mullite sol has a lower molar concentration; the amount of water added for hydrolysis during the stages of sol formation and gelation is different; and no acid catalyst is employed during the formation of the mullite precursor sol. 105 g ethanol was added to 1.5 g water in a flask. To this mixture, 30.8 g aluminum sec-butoxide (ASB) was added, and the solution was shaken to form a white slurry. This white slurry converted to a clear, water-like liquid within 12 h when kept at 55°C, and is termed as the alumina precursor sol.

Two different mullite sols were obtained: To about 60 cc alumina precursor sol, either 2.23 cc tetramethoxysilane (TMOS) or 3.35 cc tetraethoxysilane (TEOS) was added. Then, 0.27 cc water mixed with 50 cc ethanol was added to produce a clear, water-like liquid and is referred to as the mullite precursor sol. The mullite precursor sol obtained from the ASB/TMOS formulation

8

Fig. 3. Oxide interface concept for a fiber-reinforced ceramic matrix composite.
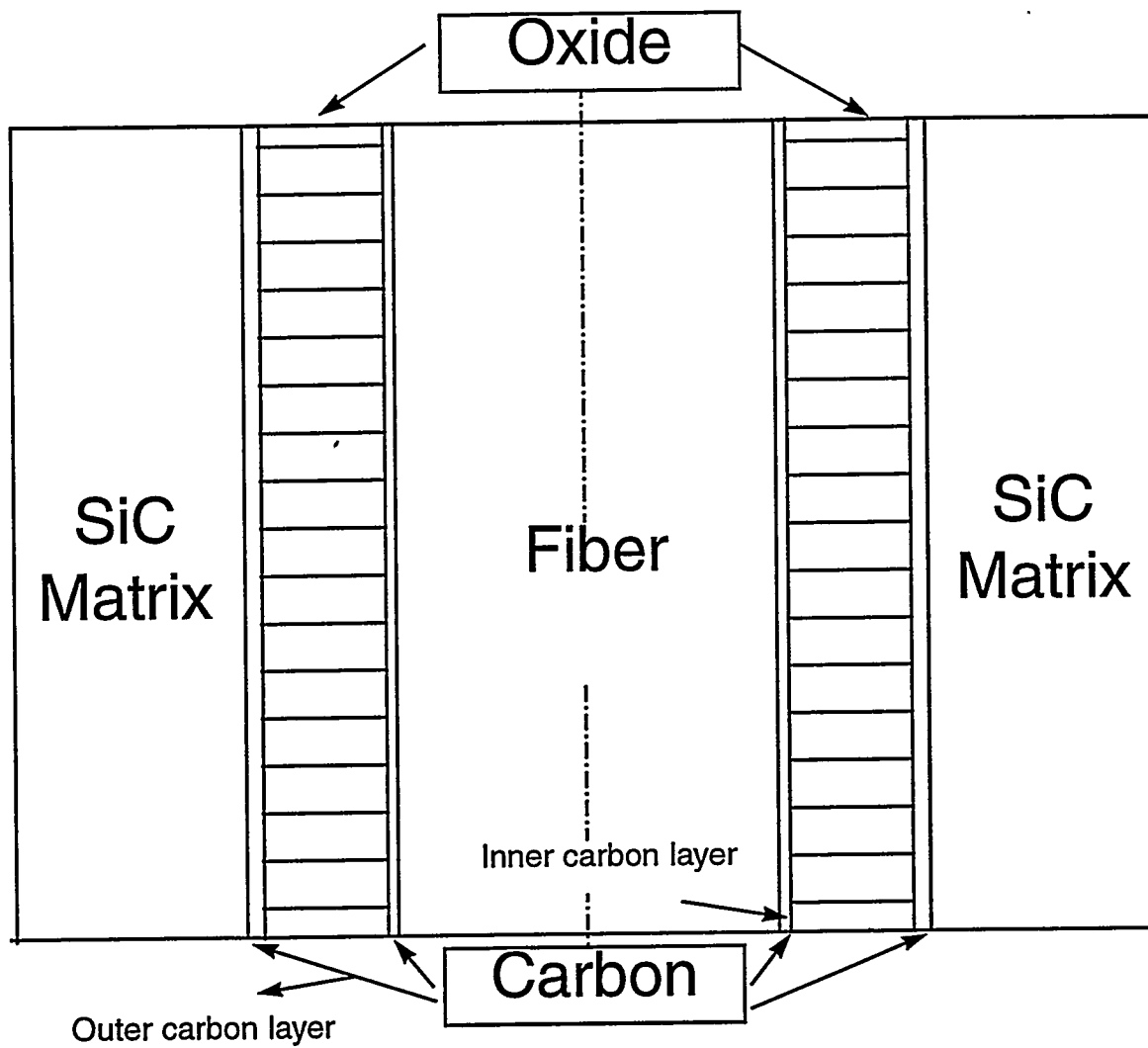
Inner Carbon Layer - Protects the fiber during the sol-gel processing of the oxide

Outer Carbon Layer - Protects the oxide coating from HCl attack during the chemical vapor infiltration processing of the SiC Matrix

and the ASB/TEOS combination are termed as MI and MII, respectively. For gelation studies, 2.71 cc water in 25 cc ethanol was then poured into each of the mullite sols (MI and MII) and gelled at 60°C. This gel was dried at 60°C for 168 h. The process procedure is summarized in Fig. 4. Additionally, aluminosilicate precursor sols with final alumina/silica ratios of 0.75 and 3 were synthesized using the ASB/TEOS combination. The following recipe was used for preparing the mullite precursor sol for coating virgin or C-coated Nicalon preforms: alumina sol-60 cc, TEOS-3.35 cc, distilled water-0.4 cc, and ethanol-50 cc.

3.2. Aluminum Titanate Precursor Sol

For synthesizing the aluminum titanate precursor sol, 10 cc titanium ethoxide (TEOD) was first dissolved in 40 cc 2-methoxyethanol. 23.62 cc of the above mixture was then poured into 60 cc of the alumina precursor sol. Next, 0.27 cc water in 50 cc ethanol was added to produce a aluminum titanate precursor sol. For gelation studies, 3.25 cc water in 25 cc ethanol was poured into the aluminum titanate sol and gelled and dried at 60°C for 168 h. The process flowchart is summarized in Fig. 5. The following recipe was used for preparing the aluminum titanate precursor sol for coating virgin or C-coated Nicalon preforms: alumina sol-80 cc, TEOD in 2-methoxyethanol-25.76 cc, distilled water-1 cc, and ethanol-100 cc.

3.3. Gel Characterization

3.3.1. Differential Scanning Calorimetry

Differential scanning calorimetry (DSC) runs were conducted in a Pt crucible with sapphire (45 mg) as the reference material and about 40-50 mg of the precursor powder obtained from the gel as the test sample. The DSC furnace was ramped at 20°C/min between 20°C and 1450°C, and the measurements were conducted in air.

3.3.2. High-Temperature X-ray Diffraction

High-temperature X-ray diffraction (XRD) patterns were obtained using a Scintag PAD X θ/θ diffractometer equipped with a Cu X-ray tube, a Buehler high-temperature furnace and an
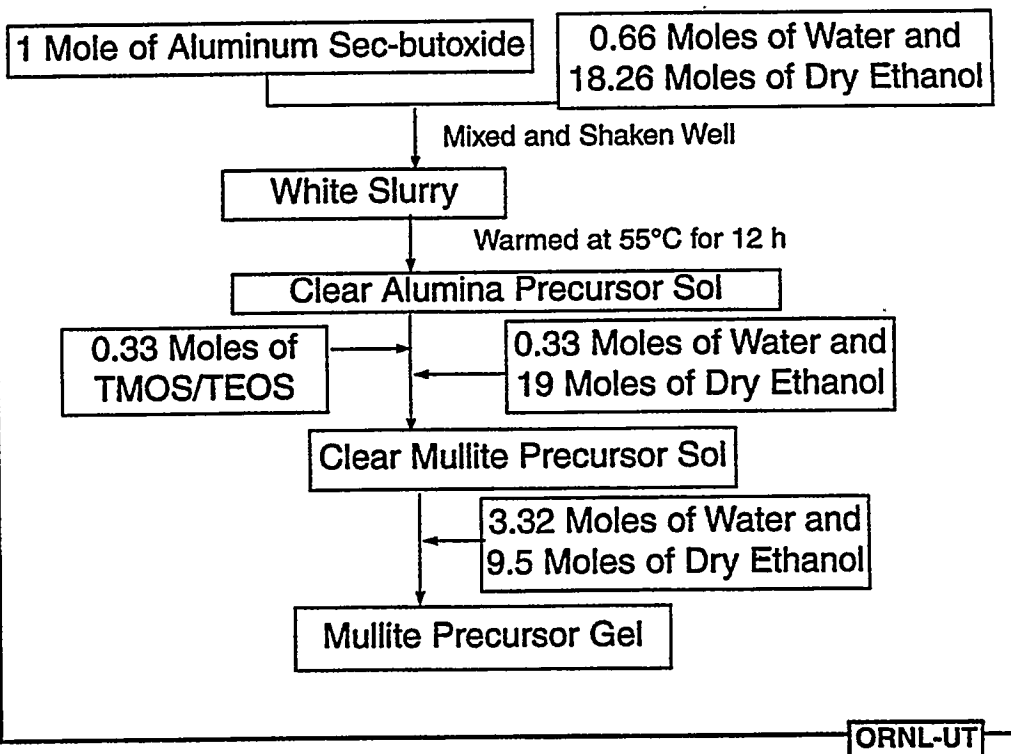
10

Synthesis of Mullite Precursor Gel (Yoldas)

| 1 Mole of Aluminum Sec-butoxide | 0.66 Moles of Water and 18.26 Moles of Dry Ethanol |

↓ Mixed and Shaken Well

White Slurry

↓ Warmed at 55°C for 12 h

Clear Alumina Precursor Sol

| 0.33 Moles of TMOS/TEOS | → | 0.33 Moles of Water and 19 Moles of Dry Ethanol |

Clear Mullite Precursor Sol

| | 3.32 Moles of Water and 9.5 Moles of Dry Ethanol |

Mullite Precursor Gel

ORNL-UT

Fig. 4 Flow diagram of the synthesis of mullite precursor gel using Yoldas' method.

11

Synthesis of Al$_2$TiO$_5$ Precursor Gel

| 1 Mole of Aluminum Sec-butoxide | 0.66 Moles of Water and 18.26 Moles of Dry Ethanol |

Mixed and Shaken Well

White Slurry

Warmed at 55°C for 12 h

Clear Alumina Precursor Sol

Water/Dry Ethanol Mixture

0.5 Moles of Titanium Ethoxide in 2 Methoxy Ethanol

Clear Al$_2$TiO$_5$ Precursor Sol

Water/ Dry Ethanol Mixture

Al$_2$TiO$_5$ Precursor Gel

ORNL-UT

Fig. 5 Flow diagram of the synthesis of aluminum titanate precursor gel.

12

mBraum position-sensitive detector. The XRD patterns were collected in a dynamic air atmosphere (100 cm^3/min) over the scan range of 20° to 70° 2θ at 5°/min and at several temperatures up to 1350°C for the mullite precursor gel and 1450°C for the aluminum titanate precursor gel. For the MI and MII mullite precursor powders, the XRD patterns were obtained at 27°C, 700°C, 750°C, 800°C, 900°C, 950°C, 1000°C, 1050°C, 1100°C, 1200°C, and 1350°C during heating, and at 50°C after cooling. Heating rates were 50°C/min up to 1100°C, and 20°C/min above 1100°C. The cooling rate was 100°C/min.

For the aluminum titanate precursor powder, the XRD patterns were obtained at 27°C, 500°C, 600°C, 700°C, 800°C, 900°C, 950°C, 1000°C, 1050°C, 1100°C, 1200°C, 1300°C, 1350°C, 1400°C, and 1450°C, during heating, and at 50°C during cooling. Heating rates were 50°C/min up to 1000°C, and 20°C/min above 1100°C. The cooling rate was 100°C/min. The obtained XRD patterns were identified by comparing with the International Centre for Diffraction Data (ICDD) patterns of mullite, α-alumina, titania, and aluminum titanate.

3.4. Nicalon Cloth and Tow Studies

Nicalon cloth (6.35 mm in diameter) was dipped in the mullite (MII) sol with concentrations ranging from 1 to 4.87 wt%, and heat treated at 1000°C for 1 h in air. Following this, the samples were examined in a scanning electron microscope to determine the coating characteristics. Nicalon tows 15 cm long were withdrawn from the 3 wt% mullite (both MI and MII) precursor sols, and aluminum titanate precursor sols at the rate of 3.7 cm/min. The coated tows were then heated in air at 1000°C for 1h or 10 h. Additionally, Nicalon tows were dip-coated in aluminosilicate sols with different alumina/silica ratios, and heat treated at 1000°C for 1 h.

3.5. Composite Fabrication

The Nicalon preform (50 layers) was prepared by stacking multiple layers of the corresponding cloth (45 mm dia) in a 0°/30°/60° sequence within the cavity of a graphite holder (12.5 mm thick). The preform was hand-compressed and held within the holder by a graphite lid.

Thin inner C coatings were deposited in some cases on the fibrous preform (prior to the oxide deposition by the sol-gel route). Thin outer C coatings were deposited on the sol-gel oxide in all cases prior to the SiC matrix infiltration. The C coating was deposited by a chemical vapor deposition process under isothermal and reduced pressure conditions. This process was conducted under the following conditions within the furnace used for chemical vapor infiltration (CVI): 1100°C, 1-2 kPa, gas flows of 25 cm^3/min propylene, and 500 cm^3/min argon for 15 min.

The mullite precursor coatings were applied either on a virgin or C-coated Nicalon preform by vacuum infiltration of the mullite precursor sol (MII) followed by drying at 110°C. This step was repeated 3-4 times till a final coating thickness of 150-300 nm was obtained (based on weight gain). Then the corresponding mullite and alumina-titania precursor-coated preforms were heat treated in argon at 1050°C for 1 h to obtain mullite and alumina-titania coatings, respectively.

The SiC matrix was infiltrated using a forced-flow CVI process developed at the Oak Ridge National Laboratory and is described elsewhere [26]. The process parameters used for the SiC infiltration are as follows: top surface temperature of 1200°C; methyltrichlorosilane flow of 0.3 g/min and hydrogen flow of 500 cm^3/min; and the exhaust pressure of 101 kPa. Typically, the SiC matrix infiltration was completed within 20 hours. Nicalon/SiC composites with the following interfaces were fabricated: (1) mullite/C interface, (2) alumina-titania/C interface, (3) C/mullite/C interface, and (4) C/alumina-titania/C interface. The basis for depositing an alumina-titania interface instead of an aluminum titanate interface would be explained in the results and discussion section.

3.6. Flexure Testing

Twenty four flexure bars of dimensions, ~ 2.5 x 3.0 x > 33 mm, were obtained from each composite disk. The geometrical density of each of the flexure bars was determined from the weight and dimension measurements of the bar.

The flexure strengths of the composites were determined at room temperature in both as-processed and after oxidation at 1000°C in air. Twelve flexure bars of each of the fabricated composites were tested in the as-processed condition. For Nicalon/SiC composites with low strength (< 150 MPa) in the as-processed condition, the remaining 12 bars were oxidized at 1000°C for 24 h in air, and subsequently tested at room temperature. In the case of composites with moderate strength (> 225 MPa) in the as-processed condition, the remaining 12 bars were oxidized at 1000°C in air as follows: 6 bars for 24 h, 3 bars for 200 h, and 3 bars for 500 h. The fracture surfaces of the as-processed and oxidized samples were examined using a scanning electron microscope.

4. RESULTS AND DISCUSSION

4.1. Gel Characterization

4.1.1. Differential Scanning Calorimetry

The DSC curve obtained from the powder derived from the mullite precursor gel, MI, is shown in Fig. 6. The DSC curves of MI and MII gel show an initial endothermic peak around 150°C corresponding to a water loss followed by two broad exothermic peaks above 220°C and below 650°C. These exothermic peaks are associated with organics being burnt out. This is followed by a sharp exothermic peak around 990°C corresponding to mullite crystallization. Further, the mullite crystallization temperature is the same for both TMOS-ASB (MI) and TEOS-ASB (MII) combinations and is similar to Yoldas' result [25]. The DSC curve obtained from an aluminum titanate precursor gel is shown in Fig. 7. An endothermic peak is observed around 150°C and corresponds to a water loss. This is followed by three exothermic peaks above 220°C and below 600°C, which correspond to the organics being burnt off. Subsequently, titania crystallizes between 700 and 900°C, and α-alumina crystallizes around 1000°C, respectively. Then alumina and titania react to form aluminum titanate between 1340°C and 1400°C (Fig. 7).
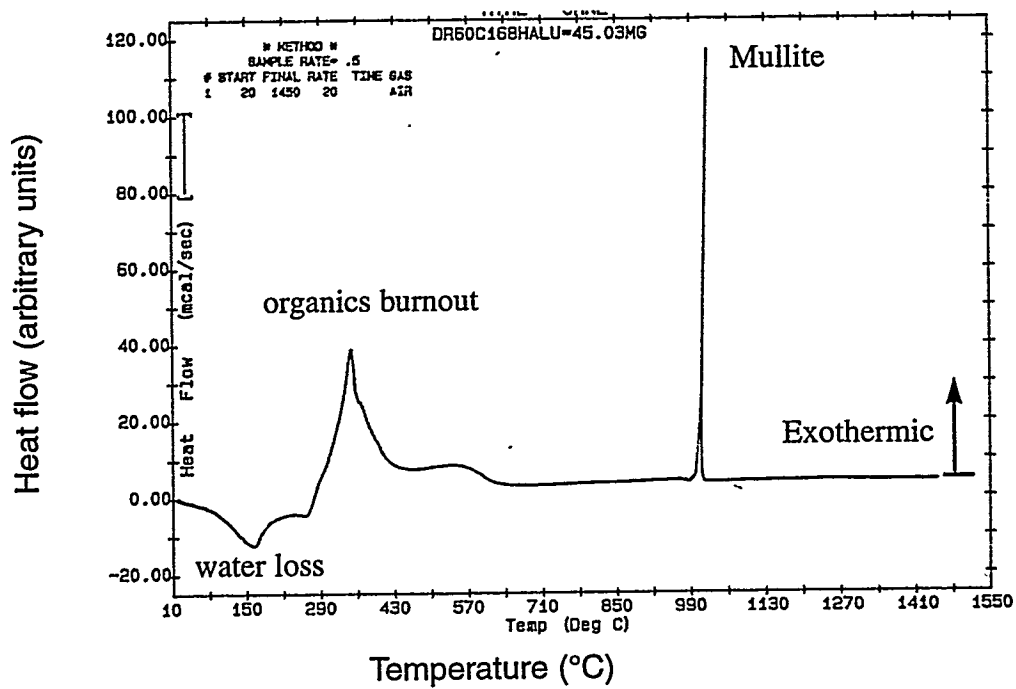
Fig. 6 DSC curve of the powder obtained from the mullite precursor gel (MI) using the ASB-TMOS combination.
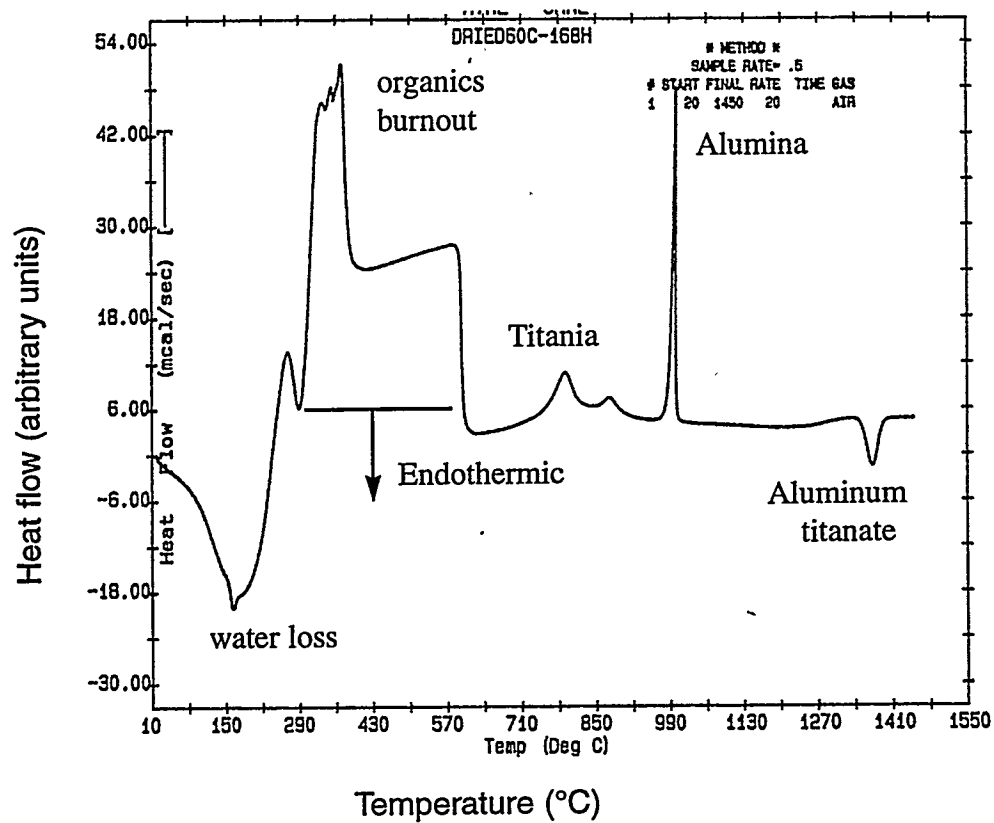
Fig. 7 DSC curve of the powder obtained from the aluminum titanate precursor gel.

17

4.1.2. High-Temperature X-ray Diffraction

High-temperature XRD patterns obtained from the MII gel derived powder is shown in Fig. 8. It is evident from Fig. 8 that at room temperature there are three peaks corresponding to the substrate Pt-Rh, and these peaks are present in the XRD patterns at all temperatures. From room temperature to 1000°C, only the substrate peaks are present. At 1050°C, mullite peaks are present in addition to the substrate peaks, and match well with the ICDD pattern for mullite. These mullite peaks continue to be present till 1350°C (# 11 in Fig. 8) and can be quenched to 50°C (# 12 in Fig. 8). Similar evolution of the mullite peaks (at 1050°C) is observed from the powder derived from the MI gel, and earlier, Yoldas' [25] made similar observation. Hence, if a Nicalon cloth is dip-coated at room temperature, dried, and heat treated at 1050°C in air, a mullite coating can be obtained. The mullite crystallization temperature is not high enough to cause degradation of Nicalon fibers.

The high-temperature XRD results are consistent with the DSC results (Fig. 7) for aluminum titanate. The high-temperature XRD patterns also show that titania cystallization occurs at 900°C followed by alumina crystallization at 1000°C (Fig. 9). Alumina and titania then react to form aluminum titanate around 1400°C. This formation temperature is very high and would degrade Nicalon fibers. Additionally, residual amounts of alumina and titania remain at 1400°C.

4.2. Nicalon Cloth and Tow Studies

Mullite coatings were applied on Nicalon cloth by dip-coating in sols of different wt% yield of mullite. These studies indicate that better coatings are obtained at 1 to 3 wt% yield of the oxide coating sol than from the 4.87 wt% oxide yield sol. The room-temperature XRD pattern of a Nicalon cloth dip-coated in a mullite sol and heat treated at 1050°C in air for 30 min indicates that mullite was deposited. Coated Nicalon tows were used to determine whether Nicalon is damaged during sol-gel processing. Nicalon tows were dip-coated in a mullite sol (MII) at various withdrawal rates, and a slow withdrawal rate (3.7 cm/min) resulted in thin (< 100 nm) and much
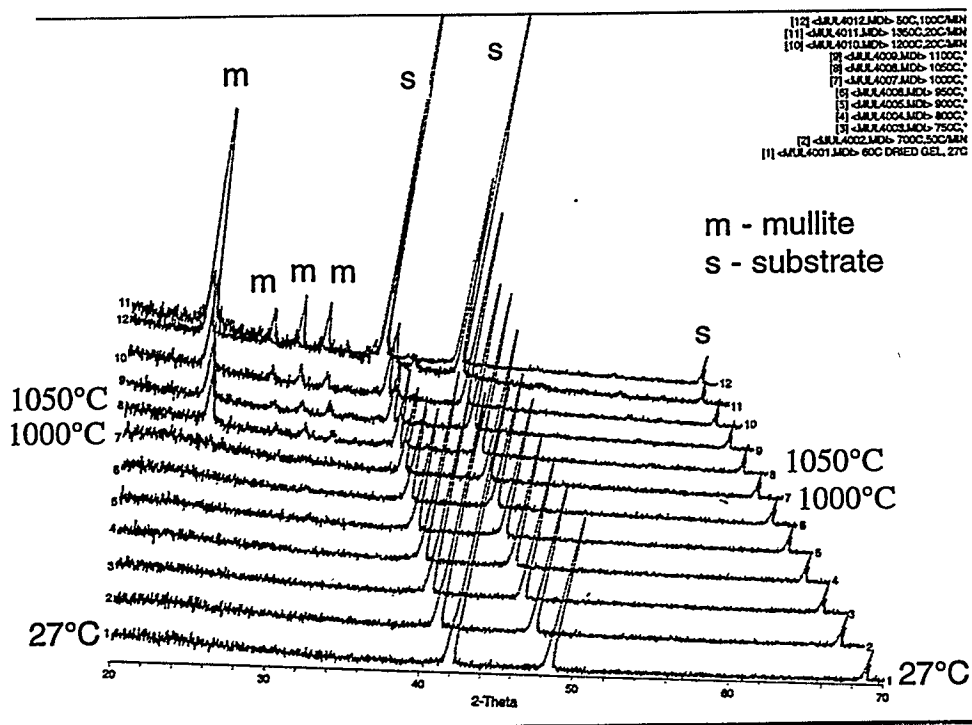
Fig. 8 High-temperature XRD patterns show that mullite crystallization occurs at 1050°C from the MII mullite precursor gel.
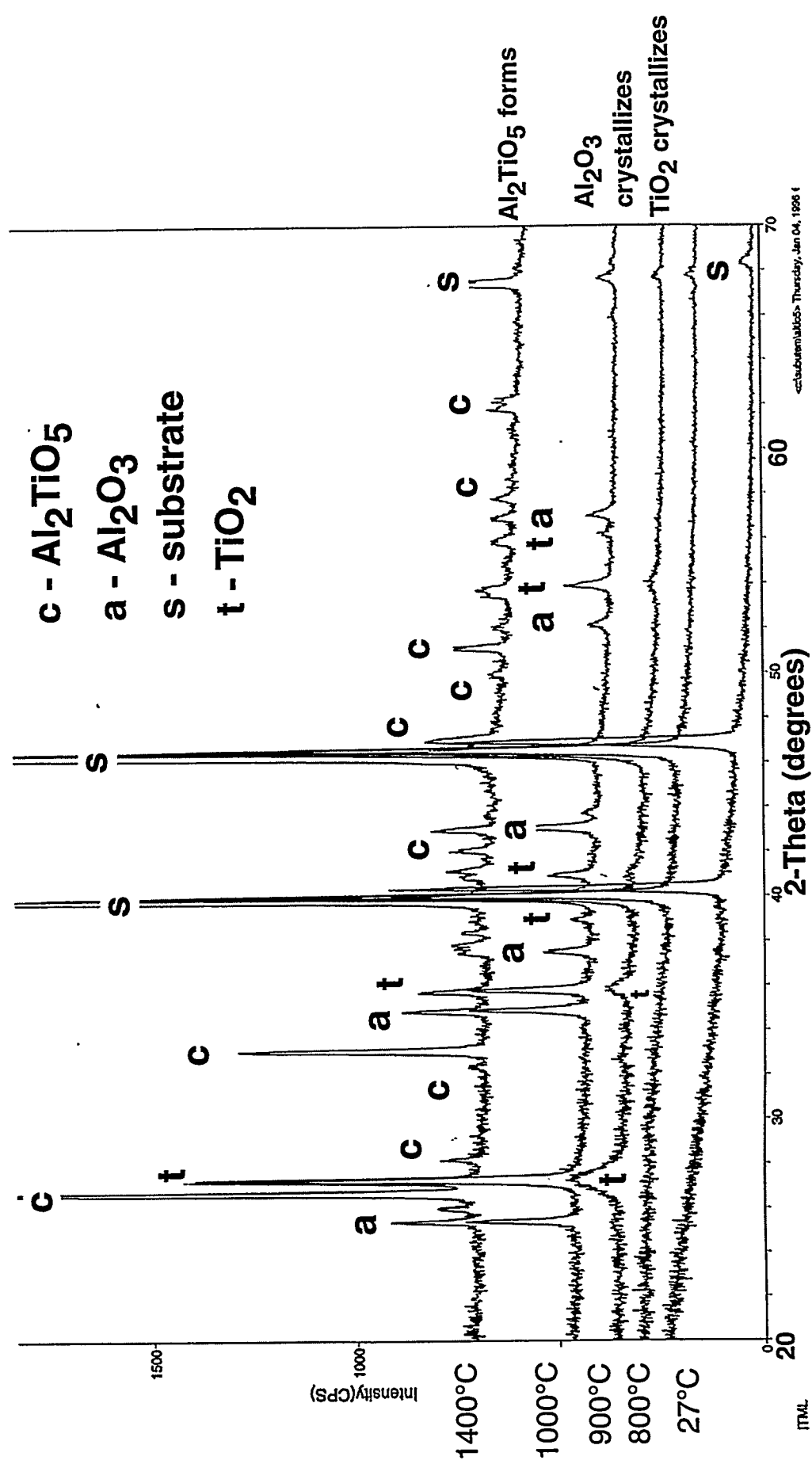
Fig. 9 High-temperature XRD patterns indicate that aluminum titanate forms at 1400°C.

more uniform coatings than other withdrawal rates (> 3.7 cm/min). Figure 10 shows a secondary electron image of a mullite coating on a Nicalon tow heat treated at 1000°C along with an energy dispersive X-ray (EDX) spectrum. The EDX analysis (not shown here) indicates that the relative intensity of aluminum to silicon peaks varies from one region to another in the tow.

Nicalon tows coated with a mullite (MI) sol and heat treated at 1000°C for 1 h in air had poor handleability, thus, suggesting that the coated tows were embrittled. In contrast, Nicalon tows coated with a mullite sol obtained from the ASB/TEOS (MII) formulation and similarly heat treated had better handleability. However, longer heating times (10 h) in air resulted in poor handleability.

The tows dip-coated in an aluminosilicate precursor sol with a lower alumina/silica ratio of 0.75 and heat treated at 1000°C in air were less handleable than those dip-coated in a mullite sol (MII). In contrast, the tows dip-coated in an aluminosilicate precursor sol with a high alumina/silica ratio of 3 had good handleability. At the present time, the quantitative measurement of the strength of the fibers before and after coating has not been measured.

Figure 11 shows a secondary electron image and an EDX spectrum of Nicalon tows coated with the aluminum titanate precursor sol and heat treated at 1000°C for 1 h in air. It should be noted that only an alumina and titania mixture would form on Nicalon under this condition. The coated Nicalon tows had good handleability, and this persisted even after longer heating times (10 h) in air. *Since the alumina-titania mixture did not damage the fiber tows at 1000°C, it was decided that alumina-titania coating would be pursued as an interface coating instead of aluminum titanate.* It should be noted that the calculated modulus of the alumina-titania mixture is 331 GPa. Although alumina-titania is a high modulus material, it was selected because of the ability to process this coating without damaging the handleability of the fiber after sol-gel processing.
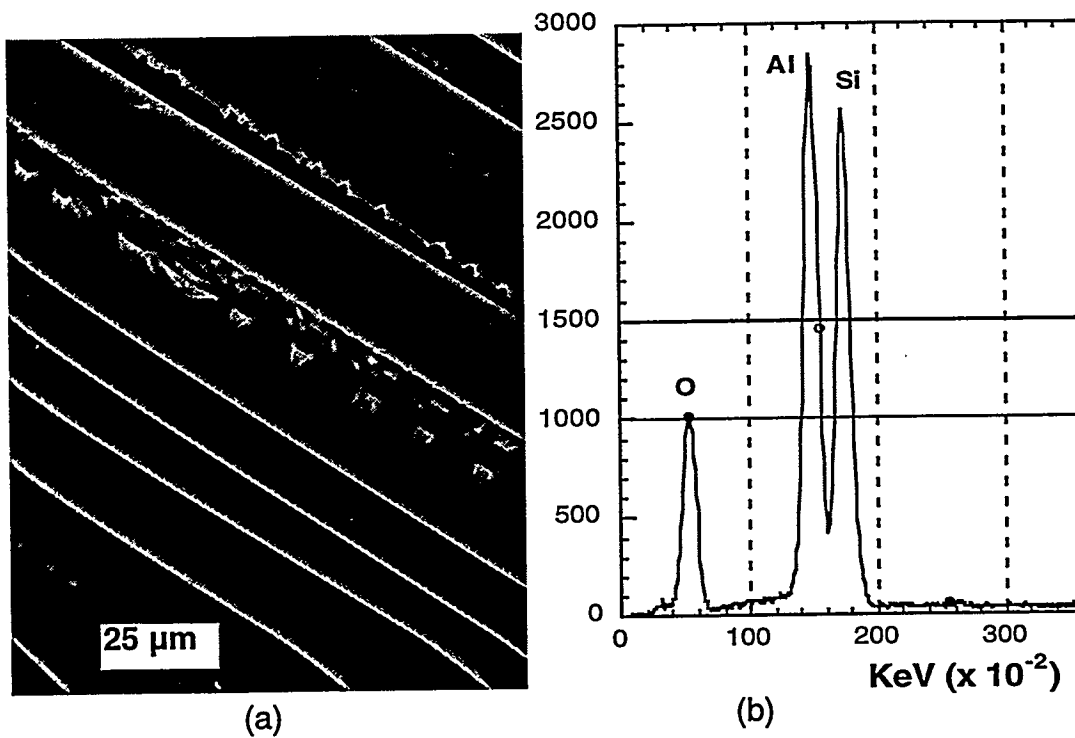
Fig. 10 Mullite coating on a Nicalon tow heat treated at 1000°C
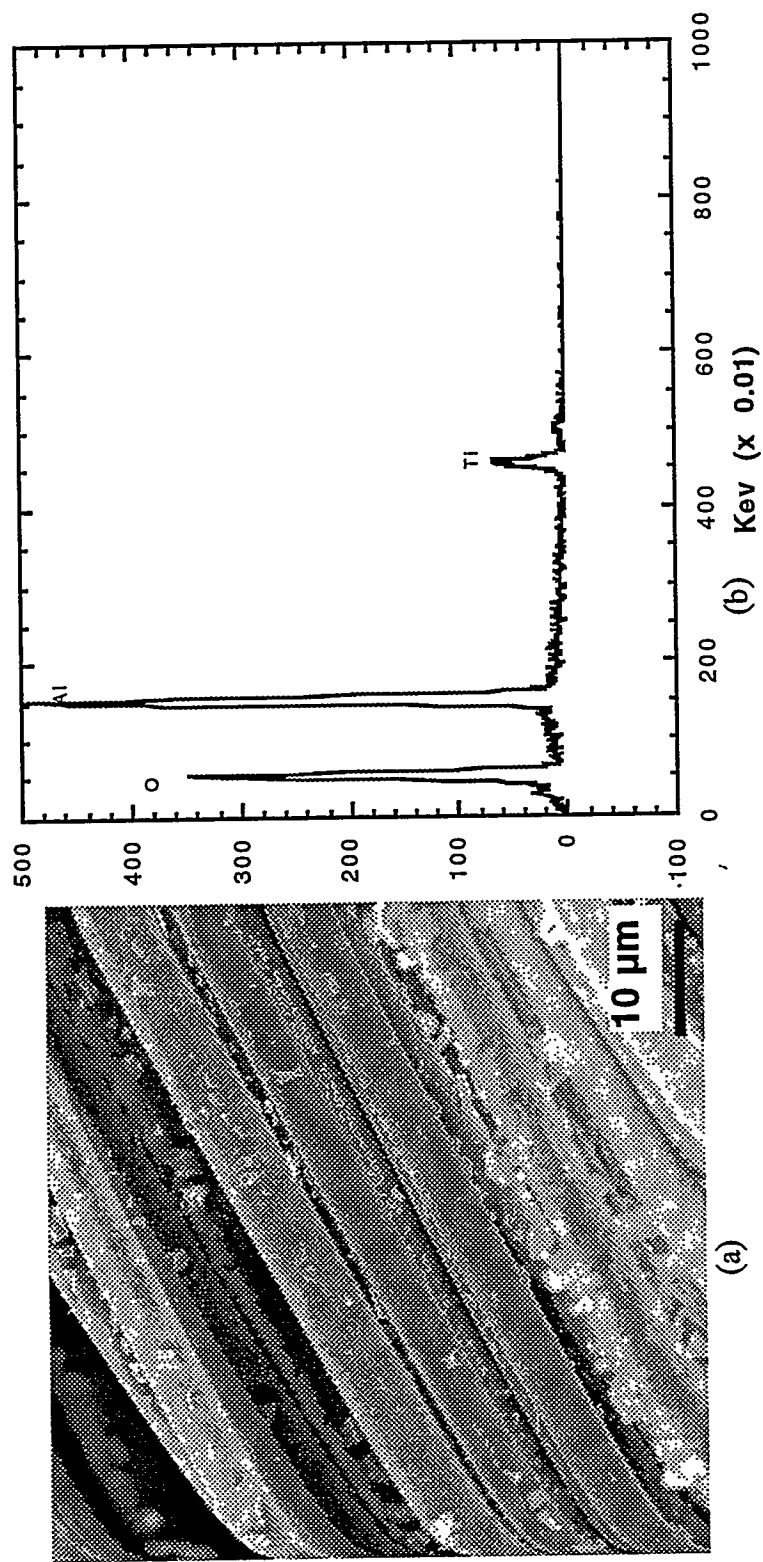(a) a secondary electron image (b) an EDX spectrum

Fig. 11 An alumina-titania coating on a Nicalon tow heat treated at 1000°C
(a) a secondary electron image(b) an EDX spectrum

23

4.3. Flexure Testing

Table 3 summarizes the fabricated Nicalon/SiC composites with four different interfaces along with their densities and interface coating thicknesses calculated from weight gain measurements. The flexure strength results of Nicalon/SiC composites with four different interfaces are summarized in Table 4. The damage-tolerant behavior represented in Table 4 and the discussion below corresponds to the composite exhibiting multiple matrix cracking, interface debonding, crack deflection, fiber fracture and fiber slip and pullout. For the first two composites in Table 4, there was no inner C layer between the fiber and the oxide, while the last two composites had an inner C layer (Fig. 3). From Table 4, it is evident that composites without an inner C layer had low flexure strength ($\leq$ 122 MPa). The composite with a mullite/C interface had low flexure strengths ($\leq$ 80 MPa) both in the as-processed and oxidized condition, and underwent brittle failure (no damage-tolerance). This could be attributed to the fiber degradation during the sol-gel processing of the oxide on the fiber since the Nicalon tows with mullite coating had poor handleability within 10 h oxidation at 1000°C (as mentioned earlier). In contrast, the composite with an Al_2O_3-TiO_2/C interface displayed damage-tolerant (non-catastrophic failure) behavior in both as-processed and oxidized conditions, but with low flexure strengths ($\leq$ 122 MPa). The damage-tolerant behavior is consistent with the earlier observation that the Nicalon tows with an alumina-titania coating had good handleability even after 10 h oxidation at 1000°C in air. The two composites discussed above highlights that a good handleability of the fiber with the coating may also be an important criterion in influencing its composite behavior.

The composite with a C/mullite/C interface had a moderate flexure strength of 268 MPa in the as-processed condition and retained almost the same strength even after 24 h oxidation. However, the strength dropped to 200 MPa after 200 h oxidation and did not undergo significant reduction even after 500 h oxidation. This composite had damage-tolerant behavior in the as-processed condition and maintained this characteristic even after 500 h oxidation.

24

Table 3. Density and interface coating thicknesses of the fabricated Nicalon/SiC composites

CVI#	Interface	Theoretical Density	Density (g/cm^3)	Interface Coating Thickness (nm)*		
				Inner Carbon	Oxide	Outer Carbon
982	Mullite/C	2.92	2.33±0.06	-	272	11
985	Al_2O_3–TiO_2/C	2.94	2.41±0.05	-	174	33
986	C/Mullite/C	2.92	2.47±0.06	22	204	21
1002	C/ Al_2O_3–TiO_2/C	2.94	2.46±0.06	28	163	27

* Calculated from weight gain

Table 4. Flexure strength results of Nicalon/SiC composites with four different interfaces

| CVI# | Interface | Density (g/cm^3) | Flexure Strength (MPa) | | | | Fracture Type |
| | | | As-Processed | Oxidized at 1000°C in air | | | |
				24 h	200 h	500 h	
982	Mullite/C	2.33±0.06	64±8*	80±9*	-	-	Brittle
985	Al_2O_3-TiO_2/C	2.41±0.05	122±29*	112±24*	-	-	Damage-tolerant
986	C/Mullite/C	2.47±0.06	268±52*	260±61**	200±47***	184±28***	Damage-tolerant
1002	C/ Al_2O_3-TiO_2/C	2.46±0.06	255±35*	189±45***	217±35***	159±20***	Damage-tolerant

* 12 flexure bars   ** 6 flexure bars   *** 3 flexure bars

26

In the as-processed condition, the composite with a C/Al$_2$O$_3$-TiO$_2$/C interface had a higher flexure strength (255 MPa) than the composite with an Al$_2$O$_3$-TiO$_2$/C interface (122 MPa). The composite with a C/Al$_2$O$_3$-TiO$_2$/C interface continued to exhibit damage-tolerant behavior even after 500 h oxidation but with a flexure strength of 159 MPa. Figures 12 (a), and (b) show the load versus displacement curve for samples in the as-processed and after 500 h oxidation for composites with a C/mullite/C interface and a C/Al$_2$O$_3$-TiO$_2$/C interface, respectively. It is evident from the figure that even after 500 h oxidation, these samples displayed a non-catastrophic mode of failure.

4.4. Scanning Electron Microscopy (SEM)

The fracture surface examination of the Nicalon/SiC composite with a mullite/C interface and alumina-titania/C interface showed very little fiber pullout, which corresponds well with the low flexure strengths of these composites (Table 4). Figure 13 shows a fracture surface of the Nicalon/SiC composite with an alumina-titania/C interface exhibiting limited fiber pullout. In contrast, the Nicalon/SiC composites with a C/alumina/titania/C interface and C/mullite/C interface exhibited considerable amounts of fiber pullout (Figs. 14 and 15). Figures 14 (a) and (b) show a Nicalon/SiC composite with a C/alumina-titania/C interface in the as-processed condition and after oxidation for 500 h at 1000°C in air. The moderate flexure strength (255 MPa) exhibited by this composite in the as-processed condition is consistent with the observation of a considerable amount of fiber pullout in Fig. 14 (a). After oxidation, this composite exhibited reduced fiber pullout (Fig. 14 (b)). Figure 15 shows a Nicalon/SiC composite with a C/mullite/C interface displaying a substantial amount of fiber pullout even after 500 h oxidation at 1000°C in air.

The manufacturer's Nicalon fiber data sheet indicates that the fiber tensile strength decreases from 1.90 GPa at room temperature to 1.32 GPa (~ 31% reduction) after oxidation for 500 h at 1000°C in air. Preliminary fiber fracture surface examination shows that pits are formed on the fiber surface after 500 h oxidation of the Nicalon/SiC composite with a C/alumina-titania/C
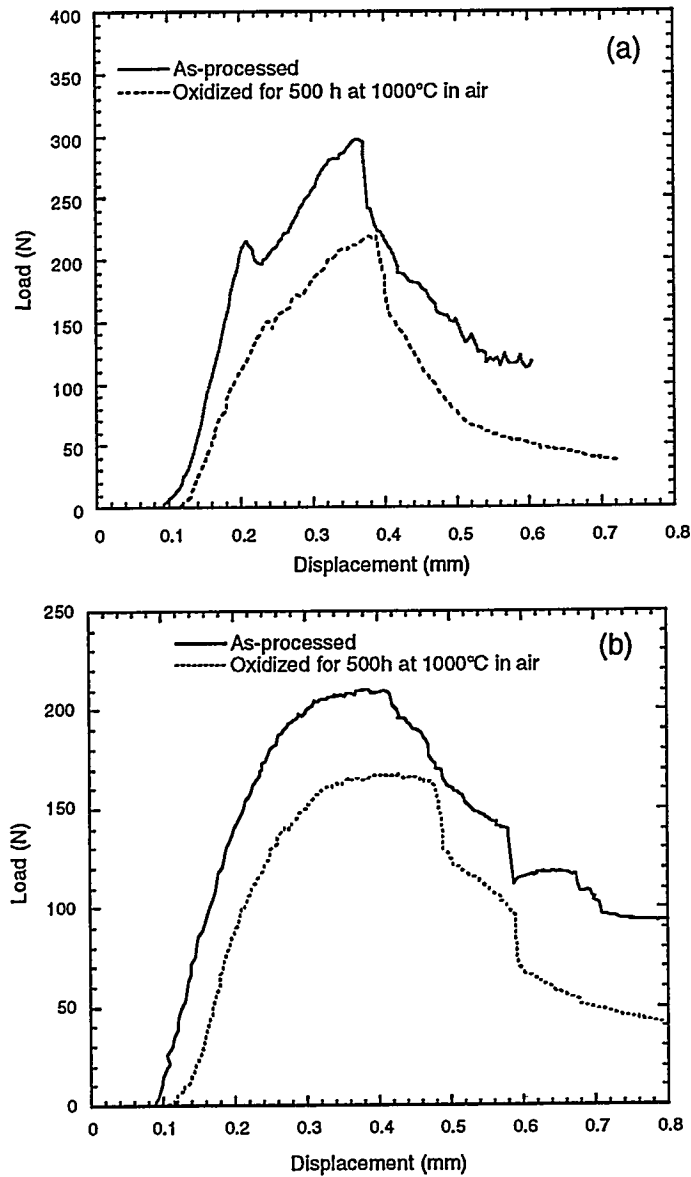
Fig.12 Flexure curves for Nicalon/SiC composites with (a) C/mullite/C interface and (b) C/alumina-titania/C interface. Both composites show damage-tolerant behavior even after 500 h oxidation at 1000°C in air.
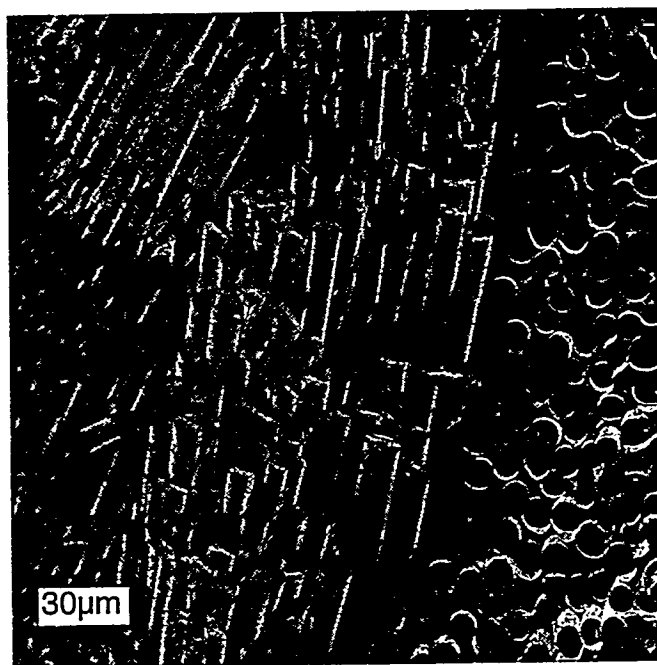
28

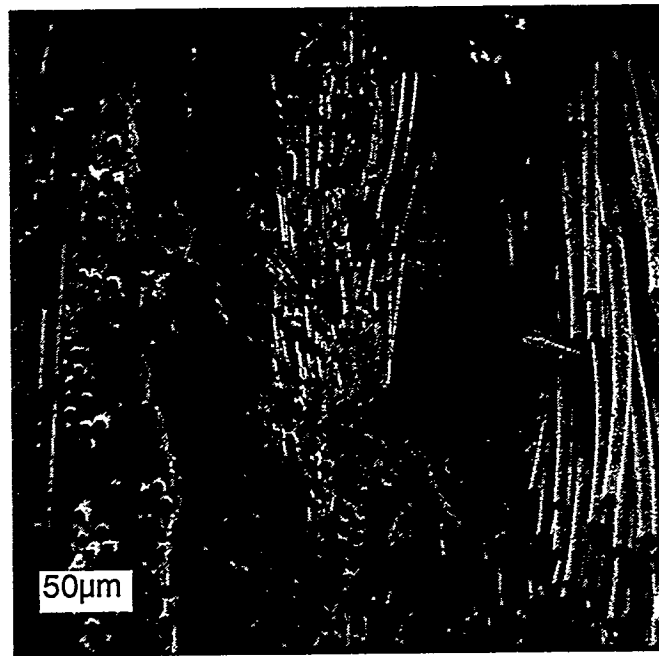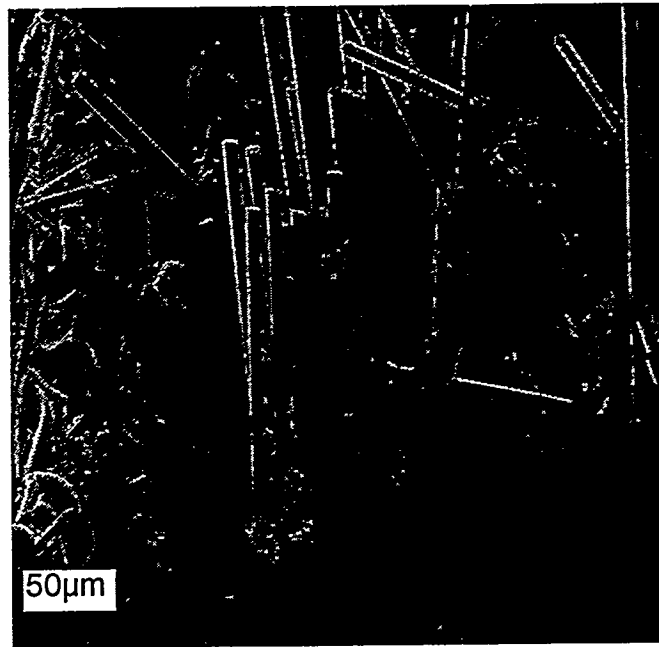Fig. 13 Nicalon/SiC composite with an alumina-titania/C interface exhibited little fiber pullout.

29

Fig. 14 Nicalon/SiC composite with a C/alumina-titania/C interface
(a) As-processed condition - Substantial amount of fiber pullout
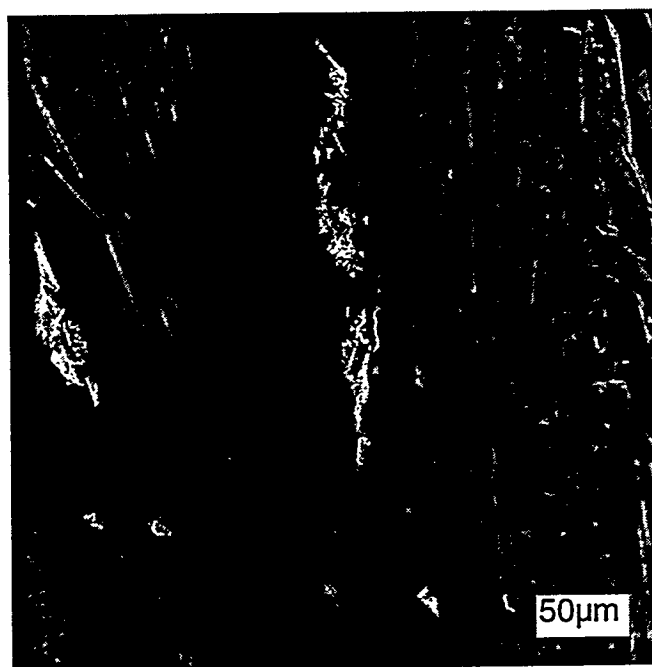(b) Oxidized for 500 h at 1000°C in air - Reduced fiber pullout

30

Fig. 15 Nicalon/SiC composite with a C/mullite/C interface exhibited substantial amount of fiber pullout even after 500 h oxidation.

interface at 1000°C (Fig. 16). Consequently, the observed loss in flexure strength after oxidation (about 38% reduction) of the composite may be due to fiber degradation, and not by virtue of interface degradation. Detailed SEM and transmission electron microscopy studies are currently being conducted to determine the extent of fiber damage and interface coating thickness, respectively. Auger electron microscopy studies are also being conducted to determine where the debonding occurred.

5. CONCLUSIONS

Mullite and aluminum titanate precursor sols were developed for Nicalon fiber coating applications. High-temperature X-ray diffraction studies identified that mullite crystallization and aluminum titanate formation occurred around 1050°C and 1400°C, respectively. Since aluminum titanate forms at 1400°C, it is not possible to deposit it on Nicalon fibers without damaging them. Nicalon tows with an alumina-titania coating mixture had good handleability even after exposure to 1000°C for 10 h in air. Consequently, an alumina-titania interface coating was pursued instead of aluminum titanate. However, Nicalon tows with a mullite coating had poor handleability after exposure to 1000°C for 10 h. As a result, the need to protect the fiber by means of a C coating prior to the oxide deposition was recognized.

Nicalon/SiC composites with C/oxide/C (the oxide interface concept) interfaces exhibited higher flexure strengths and retained damage-tolerant behavior even after 500 h at 1000°C than those of composites with oxide/C interfaces. Among the composites investigated, the composite with a C/mullite/C interface had the highest flexure strength in the as-processed condition and after 500 h oxidation at 1000°C. The good handleability of the fiber with the coating after processing may be an important indicator of the subsequent composite behavior. Efforts to replace C or BN interfaces with oxidation-resistant interface materials, such as C/mullite/C and C/alumina-titania/C interfaces, have met initial success. Continued development and stressed-oxidation tests of these
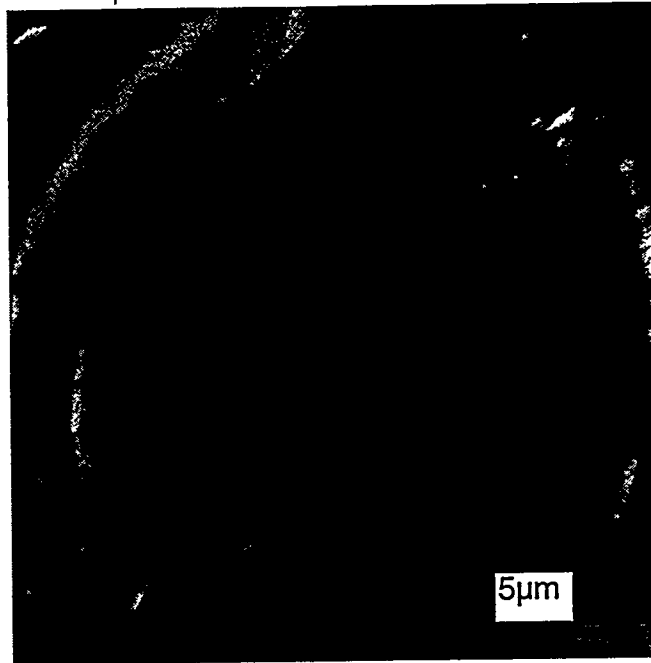
Fig. 16 Pits are formed on the Nicalon fiber surface after 500 h oxidation in air at 1000°C in a Nicalon/SiC composite with a C/alumina-titania/C interface.

composites with an oxide interface concept need to be conducted to establish their potential as a viable oxidation-resistant interface material.

6. ACKNOWLEDGMENTS

7. REFERENCES

1.   I. W. Donald and P. W. McMillan, J. Mater. Sci. **11**, 949 (1976).

2.   M. Karnitz, D. F. Craig, and S. L. Richlen, Am. Ceram. Soc. Bull. 70, 430 (1991).

3.   P. F. Becher and G. C. Wei, Mater. Sci. Eng. A107, 257 (1989).

4.   H. Kodama, T. Suzuki, H. Sakamoto, and T. Miyoshi, J. Am. Ceram. Soc. 73, 678 (1990).

5.   D. B. Marshall and A. G. Evans, J. Am. Ceram. Soc. 68 [5], 225 (1985).

6.   T. M. Besmann, B. W. Sheldon, R. A. Lowden, and D. P. Stinton, Science 253, 1104 (1991).

7.   J. K. Weddel, J. Text. Inst., 81 [4], 333 (1990).

8.   Information from fiber data sheet and personal communication from Technical Personnel of: 3M, Textron, BP, Nippon Carbon, Ube Industries, ICI, Tonen, Dow Corning, MER, Saphikon, Mitsui Mining, and Sumitomo Chemical.

9.	T. L. Tompkins, "Ceramic Oxide Fibers: Building Blocks for New Applications," Ceramic Industry, April, 1995.

10.	H. G. Sowman and D. D. Johnson, "Oxide Fibers from Chemical Ceramic Process," pp. 122-140 in Fiber Reinforced Ceramic Composites: Materials, Processing and Technology, Edited by K. S. Mazdiyasni, Noyes Publications, New Jersey, 1990.

11.	J. Persh, Ceram. Eng. Sci. Proc., 9 [7-8], 529 (1988).

12.	K. K. Chawla, Ceramic Matrix Composites, Chapman and Hall, London, 1993.

13.	R. J. Kerans, Scripta Metall. and Mater., 32, 505 (1995).

14.	R. A. Lowden, Ceram. Trans. 19, 619 (1991).

15.	S. Shanmugham, D. P. Stinton, F. Rebillat, A. Bleier, T. M. Besmann, E. Lara-Curzio, and P. K. Liaw, Ceram. Eng. Sci. Proc. 16, 389 (1995).

16.	R. Naslain, Ceram. Trans. 58, 23 (1995).

17.	P. F. Tortorelli, S. Nijhawan, L. Riester, and R. A. Lowden, Ceram. Eng. Sci. Proc. 14, 358 (1993).

18.	R. A. Lowden, O. J. Schwarz, and K. L. More, Ceram. Eng. Sci. Proc. 14, 375 (1993).

19.	R. A. Lowden, "Fiber Coatings and the Mechanical Properties of a Continuous Fiber-Reinforced SiC Matrix Composite," pp. 157-71 in Designing Ceramic Interfaces II-Understanding and Tailoring Interfaces for Coating, Composite, and Joining Applications, Proceedings of the Second European Colloquium, Edited by S. D. Peteves, Commision of the European Communities, Netherlands, 1993.

20.	R. A. Lowden and D. P. Stinton, Ceram. Eng. Sci. Proc. 9, 705 (1988).

21.	R. A. Lowden, ORNL/TM-11039, Oak Ridge National Laboratory, Oak Ridge, TN, March 1989.

22.	D. M. Walukas, "A Study of the Mechanical Properties and Oxidation Resistance of Nicalon/SiC Composites with Sol-Gel Derived Oxide Interfacial Coatings," Masters Thesis, The University of Tennessee, Knoxville, Tennessee, May 1993.

23.	C. H. Hsueh, P. F. Becher, and P. Angelini, J. Am. Ceram. Soc. 71, 929 (1988).

24.	S. Shanmugham, P. K. Liaw, D. P. Stinton, T. M. Besmann, K. L. More, A. Bleier, W. D. Porter, and S. T. Misture, in press (Ceram. Eng. Sci. Proc. 17, 1996).

25.	B. E. Yoldas, J. Mater. Sci. 27, 6667 (1992).

26.	D. P. Stinton, T. M. Besmann, and R. A. Lowden, Am. Ceram. Bull. 67, 350 (1988).

CERAMIC COMPOSITES DISTRIBUTION

3M COMPANY
Ceramic Materials Department
201-4N-01 3M Center,
St. Paul, MN 55144
M. A. Leitheiser

AIR PRODUCTS AND CHEMICALS
P.O. Box 538
Allentown, PA 18105
S. W. Dean

ALLISON GAS TURBINE DIVISION
P.O. Box 420
Indianapolis, IN 46206-0420
P. Khandelwal (Speed Code W-5)
R. A. Wenglarz (Speed Code W-16)

AMA RESEARCH & DEVELOPMENT CENTER
5950 McIntyre Street
Golden, CO 80403
T. B. Cox

ARGONNE NATIONAL LABORATORY
9700 S. Cass Avenue
Argonne, IL 60439
W. A. Ellingson
J. P. Singh

ARGONNE NATIONAL LABORATORY-WEST
P.O. Box 2528
Idaho Falls, ID 83403-2528
S. P. Henslee

BABCOCK & WILCOX
Domestic Fossil Operations
20 South Van Buren Avenue
Barberton, OH 44023
M. Gold

BRITISH COAL CORPORATION
Coal Technology Development Division
Stoke Orchard, Cheltenham
Glocestershire, England GL52 4ZG
J. Oakey

CANADA CENTER FOR MINERAL & ENERGY
TECHNOLOGY
568 Booth Street
Ottawa, Ontario
Canada K1A OG1
R. Winston Revic
Mahi Sahoo

DOE
DOE OAK RIDGE OPERATIONS
P.O.Box 2001
Oak Ridge, TN 37831
Assistant Manager for
Energy Research and Development

DOE
DOE OAK RIDGE OPERATIONS
P. O. Box 2008
Building 4500N, MS 6269
Oak Ridge, TN 37831
·M. H. Rawlins

DOE
OFFICE OF BASIC ENERGY SCIENCES
Materials Sciences Division
ER-131
19901 Germantown Road
Germantown, MD 20874-1290
H. M. Kerch

DOE
IDAHO OPERATIONS OFFICE
P. O. Box 1625
Idaho Falls, ID 83415
J. B. Malmo

DOE
MORGANTOWN ENERGY TECHNOLOGY
CENTER
P.O. Box 880
Morgantown, WV 26505
R. C. Bedick
D. C. Cicero
F. W. Crouse, Jr.
R. A. Dennis
N. T. Holcombe
W. J. Huber
T. J. McMahon
J. E. Notestein

DOE
OFFICE OF FOSSIL ENERGY
FE-72
19901 Germantown Road
Germantown, MD 20874-1290
J. P. Carr

DOE
OFFICE OF VEHICLE AND ENERGY R&D
CE-151 Forrestal Building
Washington, DC 20585
R. B. Schulz

DOE
PITTSBURGH ENERGY TECHNOLOGY
CENTER
P.O. Box 10940
Pittsburgh, PA 15236
A. L. Baldwin
G. V. McGurl
L. A. Ruth
T. M. Torkos

DOW CORNING CORPORATION
3901 S. Saginaw Road
Midland, MI 48686-0995
H. Atwell

EC TECHNOLOGIES
3614 Highpoint Drive
San Antonio, TX 78217
D. J. Kenton

ELECTRIC POWER RESEARCH INSTITUTE
P.O. Box 10412
3412 Hillview Avenue
Palo Alto, CA 94303
W. T. Bakker
J. Stringer

EUROPEAN COMMUNITIES JOINT
RESEARCH CENTRE
Petten Establishment
P.O. Box 2
1755 ZG Petten
The Netherlands
M. Van de Voorde

GA TECHNOLOGIES. INC.
P.O. Box 85608
San Diego, CA 92138
T. D. Gulden

GEORGIA INSTITUTE OF TECHNOLOGY
Materials Science & Engineering (0245)
Bunger-Henry Building, Room 276
Atlanta, GA 30332-0245
T. L. Starr

IDAHO NATIONAL ENGINEERING
LABORATORY
P. O. Box 1625
Idaho Falls, ID 83415
B. H. Rabin

LAVA CRUCIBLE-REFRACTORIES CO.
P.O. Box 278
Zelienople, PA 16063
T. Mulholland

LAWRENCE LIVERMORE NATIONAL
LABORATORY
P.O. Box 808, L-325
Livermore, CA 94550
W. A. Steele

LOS ALAMOS NATIONAL LABORATORY
P.O. Box 1663
Los Alamos, NM 87545
J. D. Katz

NATIONAL MATERIALS ADVISORY BOARD
National Research Council
2101 Constitution Avenue
Washington, DC 20418
K. M. Zwilsky

OAK RIDGE NATIONAL LABORATORY
P.O. Box 2008
Oak Ridge, TN 37831
P. T. Carlson
N. C. Cole
F. D. Johnson **(5 copies)**
R. R. Judkins
E. L. Long, Jr.
D. P. Stinton
M. R. Upton

OFFICE OF NAVAL RESEARCH
Code 431, 800 N. Quincy Street
Arlington, VA 22217
S. G. Fishman

SANDIA NATIONAL LABORATORIES
Department 6211, MS 0710
Albuquerque, NM 87185
R. J. Buss
G. A. Carlson
A. G. Sault

SHELL DEVELOPMENT COMPANY
P.O. Box 1380
Houston, TX 77251-1380
L. W. R. Dicks

TENNESSEE VALLEY AUTHORITY
Energy Demonstration & Technology
MR2N58A
Chattanooga, TN 37402-2801
C. M. Huang

THE JOHNS HOPKINS UNIVERSITY
Materials Science & Engineering
Maryland Hall
Baltimore, MD 21218
R. E. Green, Jr.

THE MATERIALS PROPERTIES COUNCIL,
INC.
United Engineering Center
345 E. Forty-Seventh Street
New York, NY 10017
M. Prager

THE NORTON COMPANY
High Performance Ceramics Division
Goddard Road
Northborough, MA 01532-1545
N. Corbin

THE TORRINGTON COMPANY
Advanced Technology Center
59 Field St.
Torrington, CT 06790
W. J. Chmura

UNION CARBIDE CORPORATION
Linde Division
P.O. Box 44
175 East Park Drive
Tonawanda, NY 14151-0044
Harry Cheung

UNITED TECHNOLOGIES RESEARCH
CENTER
MS 24, Silver Lane
East Hartford, CT 06108
K. M. Prewo

UNIVERSITY OF TENNESSEE
Dept of Materials Science and Engineering
Knoxville, TN 37996-2200
Peter Liaw

UNIVERSITY OF WASHINGTON
Department of Materials Science and
Engineering
101 Wilson, FB-10
Seattle, WA 98195
T. G. Stoebe

VIRGINIA POLYTECHNIC INSTITUTE &
STATE UNIVERSITY
Department of Materials Engineering
Blackburg, VA 24601
W. A. Curtin
K. L. Reifsnider

WESTERN RESEARCH INSTITUTE
365 N. 9th Street
P.O. Box 3395
University Station
Laramie, WY 82071
V. K. Sethi

WESTINGHOUSE ELECTRIC CORPORATION
Research and Development Center
1310 Beulah Road
Pittsburgh, PA 15235
S. C. Singhal